

EFFICIENT BAYESIAN INFERENCE FROM NOISY PAIRWISE COMPARISONS

000
001
002
003
004
005 **Anonymous authors**
006 Paper under double-blind review
007
008
009
010

ABSTRACT

011 Evaluating generative models is challenging because standard metrics often fail
012 to reflect human preferences. Human evaluations are more reliable but costly and
013 noisy, as participants vary in expertise, attention, and diligence. Pairwise com-
014 parisons improve consistency, yet aggregating them into overall quality scores
015 requires careful modeling. Bradley-Terry-based methods update item scores from
016 comparisons, but existing approaches either ignore rater variability or lack conver-
017 gence guarantees, limiting robustness and interpretability. We introduce BBQ, a
018 Bayesian Bradley-Terry variant that explicitly models rater quality, downweight-
019 ing or removing unreliable participants, and provides guaranteed monotonic like-
020 lihood convergence through an Expectation-Maximization algorithm. Empirical
021 results show that BBQ achieves faster convergence, well-calibrated uncertainty
022 estimates, and more robust, interpretable rankings compared to baseline Bradley-
023 Terry models, even with noisy or crowdsourced raters. This framework enables
024 more reliable and cost-effective human evaluation of generative models.
025
026

1 INTRODUCTION

027 Evaluating generative models is challenging, particularly for large language models (LLMs) and
028 image generators, where standard metrics often fail to reflect human preferences. Metrics such
029 as BLEU (Papineni et al., 2002) and perplexity (Jelinek, 1998) for LLMs, or PSNR (Gonzalez,
030 2009), MS-SSIM (Wang et al., 2003), and FID (Heusel et al., 2017) for image models, provide
031 only limited insight into perceived quality (Mentzer et al., 2020; CLIC, 2025; Chiang et al., 2024).
032 As a result, human evaluations remain indispensable for establishing meaningful rankings between
033 models. Accordingly, leaderboards and comparative studies of large language models and Learned
034 Image Compression (LIC) methods place strong emphasis on human preference data.
035

036 However, human evaluations are expensive and time-consuming, making it crucial to design proto-
037 cols that are efficient while minimizing subjectivity and noise. In this context, pairwise comparisons,
038 in which participants choose between two items rather than providing absolute scores, represent an
039 effective and practical form of human evaluation (Zerman et al., 2018; Wang et al., 2023). They
040 are generally easier for participants and produce more consistent judgments. Collecting all pairwise
041 comparisons is infeasible because the number of pairs grows quadratically with the number of items.
042 With only a limited set of comparisons, simple statistics such as win rates are not sufficient to derive
043 overall quality scores, because a win rate depends on the quality of the items it is compared against.
044

045 To produce an overall ranking that can be displayed on leaderboards, pairwise comparisons must be
046 aggregated effectively. This motivates the development of robust and efficient aggregation methods.
047 The Bradley-Terry (BT) (Bradley & Terry, 1952) model addresses this problem by iteratively updat-
048 ing item scores based on comparison outcomes. It has become a standard approach for aggregating
049 pairwise judgments across domains.
050

051 Despite its usefulness, the standard Bradley-Terry model has several limitations in practice. There
052 are multiple algorithms for estimating BT parameters, including iterative scaling methods (Ford Jr,
053 1957), gradient descent, and the minorization maximization (MM) algorithm (Hunter, 2004). The
054 MM algorithm guarantees convergence to the global maximum for the basic BT model, whereas
055 gradient-based methods, which are closely related to the Elo rating system, are widely used in prac-
056 tice but provide no such guarantees (Hunter, 2004). For extended BT models that incorporate factors
057 such as home field advantage (Agresti, 2010), multiple comparisons (Plackett, 1975; Luce et al.,
058

054 1959), or ties (Rao & Kupper, 1967), even MM algorithms may converge only to local optima
 055 (Hunter, 2004). A further challenge is that human evaluations are inherently noisy: participants may
 056 rush, guess, or lose focus, leading to uneven reliability across raters. If such variability is ignored,
 057 unreliable raters can distort item scores and reduce ranking stability.

058 We propose a Bayesian Bradley–Terry variant that jointly models item quality and rater reliabil-
 059 ity. To the best of our knowledge, no prior work combines the BT framework with a Bayesian
 060 formulation that explicitly models rater quality and provides closed-form EM updates. Previous
 061 approaches that account for noisy raters typically rely on gradient-based optimization without con-
 062 vergence guarantees, whereas our method ensures stable convergence and yields interpretable pa-
 063 rameters. The Bayesian framework addresses epistemic uncertainty, provides regularization, and
 064 ensures stable convergence of the estimation procedure. To capture variability in participant behav-
 065 ior, our method introduces rater-specific parameters that reflect how consistent or trustworthy each
 066 participant is, allowing the model to adjust the influence of individual comparisons. We derive an
 067 EM algorithm that efficiently estimates item and rater parameters via a latent-variable formulation,
 068 guaranteeing monotonic likelihood improvement. This approach allows partially reliable raters to
 069 contribute meaningful information while reducing the impact of inattentive or inconsistent partici-
 070 pants. The Bayesian priors further regularize the estimates, preventing overfitting when many raters
 071 and parameters are involved, and leading to stable and generalizable score estimates. By modeling
 072 rater quality and adopting a Bayesian framework, our method also provides uncertainty estimates
 073 for item scores, facilitating more interpretable rankings and robust comparisons across studies.

074 We demonstrate the effectiveness of our approach on human evaluation datasets for generative mod-
 075 els, showing faster convergence, improved robustness to noisy comparisons, and more consistent
 076 rankings compared to standard BT and naive aggregation methods. Beyond generative model eval-
 077 uation, our framework can be applied to any scenario where noisy pairwise comparisons must be
 078 converted into reliable global rankings. Overall, our work contributes to more cost-efficient, inter-
 079 pretable, and reproducible human studies for evaluating AI-generated content.

080 2 RELATED WORK

081 Human studies often require ranking items. Presenting participants with a choice between two
 082 items rather than a single item with a score increases sensitivity to subtle differences and reduces
 083 variability in responses (Zerman et al., 2018; Wang et al., 2023). Consequently, many leaderboards
 084 for machine learning models rely on pairwise comparisons. In such setups, participants indicate their
 085 preference between two alternatives, and these preferences are then aggregated to produce overall
 086 rankings. Notable examples include the Chatbot Arena (Chiang et al., 2024) and the CLIC image
 087 compression challenge (CLIC, 2025), which use pairwise comparisons and combine them using
 088 variants of the Bradley–Terry (BT) model.

089 The Bradley–Terry model (Bradley & Terry, 1952) was originally developed to rank competitors in
 090 sports. It provides a probabilistic framework to estimate the likelihood that one item is preferred
 091 over another. The model converts pairwise comparisons into a ranking, making it a cornerstone in
 092 studies across games, consumer preferences, and other applications. Several extensions have been
 093 proposed to broaden its applicability. For instance, the Plackett–Luce model generalizes the BT
 094 framework from pairwise comparisons to rankings over multiple items (Plackett, 1975; Luce et al.,
 095 1959), defining a probability distribution over permutations by multiplying successive BT probabili-
 096 ties (Luce et al., 1959). Other modifications address specific contexts, such as modeling home-field
 097 advantages (Agresti, 2010), incorporating ties (Rao & Kupper, 1967), or handling comparisons be-
 098 tween groups instead of individuals (Huang et al., 2006).

099 Maximum likelihood estimation (MLE) is commonly used to infer the parameters of the basic BT
 100 model. Zermelo (1929) introduced an iterative approach to compute these estimates, which has be-
 101 come widely adopted. Later, Lange et al. (2000) demonstrated that this procedure is a particular case
 102 of minorization–maximization (MM) algorithms, which iteratively optimize surrogate functions to
 103 reach a local maximum of the likelihood. Hunter (2004) extended MM algorithms to generalized
 104 BT models and established conditions guaranteeing convergence to the MLE. For the classical BT
 105 model, the optimization is convex, ensuring convergence to the global optimum (Hunter, 2004).
 106 However, for extensions such as home-field advantage, multiple comparisons, or ties, MM algo-
 107 rithms may converge only to a local maximum (Hunter, 2004).

108 Bayesian formulations of the BT model have been explored to incorporate prior knowledge and reg-
 109 ularization (Adams, 2005; Guiver & Snelson, 2009; Caron & Doucet, 2012). Caron & Doucet (2012)
 110 showed that MM algorithms can be interpreted as Expectation-Maximization (EM) procedures, en-
 111 abling Bayesian inference via Gibbs sampling. This formulation provides tractable complete-data
 112 likelihoods and ensures convergence of the resulting Markov Chain Monte Carlo methods. The
 113 Bayesian perspective smooths posterior estimates, reducing susceptibility to local maxima, and al-
 114 lows for uncertainty quantification in the estimated item skills.

115 Annotator quality models represent a critical extension addressing the assumption that all compari-
 116 sons are equally reliable. In crowdsourced evaluations, participant quality can vary widely, moti-
 117 vating approaches that explicitly account for annotator reliability (Chen et al., 2013). Chen et al.
 118 (2013) proposed a Bayesian model that jointly estimates both item quality and rater reliability using
 119 annotator-specific parameters. Their approach places Gaussian priors on item and rater parame-
 120 ters, and incorporates scaling factors in the likelihood to modulate individual annotator influence.
 121 They perform posterior inference using gradient-based optimization, which can be challenging in
 122 high-dimensional spaces due to potential local optima. Moreover, gradient-based methods have
 123 no guarantees of convergence. In contrast, our proposed EM-based method provides guaranteed
 124 monotonic likelihood improvement. The Elo-based rater model developed by Google Research im-
 125 plements a simplified version of this approach. It is widely used in the Challenge on Learned Image
 126 Compression (CLIC) (CLIC, 2025) and related research (Mentzer et al., 2020; Ballé et al., 2025).
 127

128 To the best of our knowledge, no prior work combines the Bradley–Terry model with a Bayesian
 129 formulation that explicitly models rater quality while also providing closed-form EM updates. In
 130 contrast to Chen et al. (2013), who use Gaussian priors and gradient-based optimization without
 131 convergence guarantees, our approach leverages conjugate priors and an EM algorithm that ensures
 132 monotonic likelihood improvement. Compared to the Elo-based rater model widely used in CLIC
 133 (CLIC, 2025), which is a simplified heuristic relying on Elo-style updates, our method provides a
 134 principled Bayesian treatment with uncertainty estimates and interpretable rater-quality parameters.

135 3 METHODOLOGY

136 3.1 BRADLEY-TERRY MODEL WITH RATER QUALITY

137 The objective of converting a set of noisy pairwise comparisons into a reliable ranking of items
 138 is a fundamental problem in machine learning and statistics. Consider a set of K items that are
 139 repeatedly compared with one another in pairs by a set of R raters. The data, which we denote as D ,
 140 consists of the outcomes of these comparisons. For two items i and j of this set, Bradley & Terry
 141 (1952) suggested the following model:

$$142 P(i \text{ beats } j) = \frac{\lambda_i}{\lambda_i + \lambda_j} \quad (1)$$

143 where $\lambda_k > 0$ is a parameter associated with item $k \in \{1, 2, \dots, K\}$ that represents its skill rating.
 144 This model provides a clear and interpretable way to infer item scores from a set of observed wins
 145 and losses. However, it operates under the simplifying assumption that all comparisons are equally
 146 reliable. In the context of human evaluation, this assumption is often violated. Participants may
 147 exhibit varying levels of expertise, attention, or diligence, leading to unreliable and inconsistent
 148 judgments.

149 To account for varying rater reliability, we introduce a rater-specific quality parameter $q_r \in [0, 1]$.
 150 Intuitively, with probability q_r , rater r makes an informed judgment following the Bradley-Terry
 151 model. With probability $1 - q_r$, the rater guesses randomly, as if flipping a fair coin between the two
 152 items. This leads to the following mixture model for the probability that rater r ranks item i above
 153 item j :

$$154 P(r \text{ ranks } i \text{ above } j) = q_r \left(\frac{\lambda_i}{\lambda_i + \lambda_j} \right) + (1 - q_r) \left(\frac{1}{2} \right) \quad (2)$$

The log-likelihood of the data is given by:

$$\log P(D \mid \lambda, q) = \sum_{r=1}^R \sum_{i=1}^K \sum_{\substack{j=1 \\ j \neq i}}^K \left[w_{r,ij} \log \left(q_r \frac{\lambda_i}{\lambda_i + \lambda_j} + (1 - q_r) \frac{1}{2} \right) + (n_{r,ij} - w_{r,ij}) \log \left(q_r \frac{\lambda_j}{\lambda_i + \lambda_j} + (1 - q_r) \frac{1}{2} \right) \right], \quad (3)$$

where $n_{r,ij}$ denotes the total number of comparisons between items i and j by rater r , and $w_{r,ij}$ is the number of times rater r ranks item i above item j . There is no closed-form maximum likelihood estimator for this likelihood function, so the optimal parameters λ and q cannot be derived analytically. While an iterative optimization method like gradient descent could be used, it offers no guarantee of convergence. On the other hand, the Expectation–Maximization (EM) algorithm avoids learning-rate tuning, and guarantees a monotonic increase of the observed-data likelihood and convergence to a stationary point (Dempster et al., 1977).

3.2 THURSTONIAN INTERPRETATION

Following Caron & Doucet (2012), we interpret the Bradley-Terry model under a Thurstonian framework (Diaconis, 1988). In this perspective, a comparison between items i and j is conceptualized as a race, where each item has a random arrival time, Y_i and Y_j , respectively. These arrival times are assumed to follow exponential distributions:

$$Y_i \sim \mathcal{E}(\lambda_i), \quad Y_j \sim \mathcal{E}(\lambda_j), \quad (4)$$

and the item with the smaller arrival time is declared the winner. This leads directly to the standard Bradley-Terry probability:

$$P(i \text{ beats } j) = P(Y_i < Y_j) = \frac{\lambda_i}{\lambda_i + \lambda_j}. \quad (5)$$

For the EM algorithm, we introduce latent variables to simplify the complete-data likelihood. First, we define an indicator variable

$$A_{r,i,i}^{(c)} \sim \text{Bernoulli}(q_r), \quad (6)$$

which denotes whether the c -th comparison of items i and j by rater r follows the Bradley-Terry model. Using these indicators, we define the latent variable $Z_{r,ij}$ as the sum of the minimal arrival times across the $n_{r,ij}$ comparisons by rater r :

$$Z_{r,ij} = \sum_{c=1}^{n_{r,ij}} A_{r,ij}^{(c)} \min(Y_i^{(c)}, Y_j^{(c)}). \quad (7)$$

Conditioned on $m_{r,ij} = \sum_{c=1}^{n_{r,ij}} A_{r,ij}^{(c)}$, the variable $Z_{r,ij}$ follows a Gamma distribution,

$$Z_{r,ij} \mid m_{r,ij} \sim \Gamma(m_{r,ij}, \lambda_i + \lambda_j), \quad (8)$$

where $\Gamma(\alpha, \beta)$ denotes the Gamma distribution with shape parameter α and inverse scale β . This Gamma-distributed latent variable formulation allows for a tractable EM update while accounting for rater-specific quality.

3.3 EXPECTATION-MAXIMIZATION UPDATES

The EM algorithm is an iterative method for finding maximum a posteriori (MAP) estimates for our model parameters, λ and q , by treating the rater's quality and the unobserved arrival times from the Thurstonian interpretation as latent variables. The algorithm is guaranteed to converge to a stationary point of the posterior distribution.

First, we specify prior distributions for the parameters. The item skills λ_k are assigned a Gamma prior, $\lambda_k \sim \Gamma(a, b)$, which is a conjugate prior for the exponential distribution. Each rater's quality parameter, q_r , is given a Beta prior, $q_r \sim B(\alpha, \beta)$.

The core of the EM algorithm is the iterative maximization of the expected complete-data log-posterior, conditioned on the current parameter estimates (λ^*, q^*) . The algorithm proceeds by alternating between two steps until convergence:

216 **E-step: Expectation** In the E-step, we compute the expected complete-data log-posterior, a function
 217 we denote as Q . This function represents the expected value of the log-posterior of all observed
 218 and latent variables, given our observed data and the current parameter estimates from the previous
 219 iteration. It is defined as:

$$220 \quad 221 \quad Q(\lambda, q \mid \lambda^*, q^*) = \mathbb{E}_{A, Z \mid D, \lambda^*, q^*} \left[\ell_c(\lambda, q; D, Z, A) + \log P(\lambda) + \log P(q) \right]. \quad (9)$$

222 The complete-data log-likelihood, ℓ_c , is further broken down into three components.

$$224 \quad \ell_c(\lambda, q; D, Z, A) = \log P(Z \mid D, A, \lambda, q) + \log P(A \mid D, \lambda, q) + \log P(D \mid \lambda, q). \quad (10)$$

226 **M-step: Maximization** This step updates the model parameters by maximizing the Q function.
 227 By leveraging the expected values from the E-step, the M-step transforms the original complex op-
 228 timization problem into simpler, closed-form updates. The key quantity that is used in both updates
 229 is the posterior probability that a given comparison from rater r follows the Bradley-Terry model.
 230 This quantity, denoted as γ , represents the weight of a rater’s judgment based on how much it aligns
 231 with the model’s current predictions. It is given by:

$$232 \quad 233 \quad \gamma_{r,ij}^{(t-1)} = \frac{q_r^{(t-1)} y_{ij}^{(t-1)}}{q_r^{(t-1)} y_{ij}^{(t-1)} + (1 - q_r^{(t-1)})^{\frac{1}{2}}}, \quad (11)$$

235 where $y_{ij}^{(t-1)} = \frac{\lambda_i^{(t-1)}}{\lambda_i^{(t-1)} + \lambda_j^{(t-1)}}$ is the Bradley-Terry probability that item i beats item j . This posterior
 236 probability γ represents our confidence that a comparison was meaningful rather than random, given
 237 the current parameter estimates. Higher γ values indicate more trustworthy comparisons.

239 The new estimate for a rater’s quality, q_r , is calculated as a weighted average. The numerator
 240 sums up the “effective number of wins” for that rater, where each win is weighted by the posterior
 241 probability (γ) that it was a meaningful, non-random judgment. This is combined with the hyper-
 242 parameters from the Beta prior to regularizing the estimate. The denominator normalizes this sum
 243 by the total number of comparisons and prior parameters. This update intuitively increases a rater’s
 244 quality score if their judgments frequently align with the model’s predictions. The update is given
 245 by:

$$246 \quad 247 \quad q_r^{(t)} = \frac{\sum_{i=1}^K \sum_{j=i+1}^K \left[w_{r,ij} \gamma_{r,ij}^{(t-1)} + w_{r,ji} \gamma_{r,ji}^{(t-1)} \right] + (\alpha - 1)}{n_r + \alpha + \beta - 2}, \quad (12)$$

248 where n_r is the total number of comparisons by rater r .

250 The new estimate for an item’s skill, λ_i , is a ratio that balances two key quantities. The numerator
 251 is a sum of the “effective wins” for item i across all raters, where each win is again weighted by
 252 the rater’s quality (γ). This term essentially represents the total positive evidence for item i . The
 253 denominator, on the other hand, accounts for the total comparisons item i was involved in, and acts
 254 as a normalizing factor. These terms are also regularized by the Gamma prior hyperparameters. The
 255 update is given by:

$$256 \quad 257 \quad \lambda_i^{(t)} = \frac{\sum_{r=1}^R \left[\sum_{j=1, j \neq i}^K w_{r,ij} \gamma_{r,ij}^{(t-1)} \right] + (a - 1)}{\sum_{j=1, j \neq i}^K \left[\sum_{r=1}^R \frac{w_{r,ij} \gamma_{r,ij}^{(t-1)} + w_{r,ji} \gamma_{r,ji}^{(t-1)}}{\lambda_i^{(t-1)} + \lambda_j^{(t-1)}} \right] + b}. \quad (13)$$

260 The derivation of the Expectation Maximization algorithm is provided in Appendix B.

263 4 EXPERIMENTAL RESULTS

265 To evaluate the performance of our **Bayesian Bradley-Terry model with rater Quality (BBQ)**, we
 266 conduct a series of experiments comparing it against two baselines: Bayesian Bradley-Terry (Bayes-
 267 BT) (Caron & Doucet, 2012) and a gradient descent-based BT model that incorporates rater quality
 268 (Crowd-BT) (Chen et al., 2013). For Crowd-BT, we use the implementation provided by Google
 269 Research (Google, 2025), which was employed both by CLIC (2025) and Ballé et al. (2025). The
 hyperparameters used in our experiments can be found in Section C.

270 We evaluate the performance of several Bradley–Terry (BT) variants across datasets, including
 271 human preference benchmarks for large language models (HUMAINE (Team, 2025), MT-Bench
 272 (Zheng et al., 2023)) and image compression (WD (Ballé et al., 2025), HiFiC (Mentzer et al., 2020),
 273 ConHa (Aczel & Wattenhofer, 2024)), as well as a newly collected inhomogeneous rater quality
 274 (IHQ) dataset from the CLIC2024 image test set (CLIC, 2025). To study the effect of rater quality,
 275 we partition the IHQ dataset into two subsets: screened and unscreened. This setup enables analysis
 276 of how low-quality, high-quality, and mixed comparisons affect model performance. Details of the
 277 IHQ dataset creation are given in Section E, and a summary of all datasets, including comparisons,
 278 raters, and items, is provided in Section D and Table 2.

279 Ground truth rankings are not available for real datasets. We first validated the models on simulated
 280 datasets, where all methods recover the same ordering as the number of samples increases. For
 281 crowd-sourced datasets, we approximate the ground truth by the ranking achieved on the whole
 282 dataset. We validate that this provides a reasonable approximation of ordering for real-world datasets
 283 by examining the top-1 item in each ranking. For all datasets except IHQ-unscreened, all three
 284 models recover the same top-ranked item. For the IHQ-unscreened dataset, Crowd-BT and Bayes-
 285 BT fail to identify the reference image as the highest-quality item, whereas BBQ succeeds.

286 A reliable aggregation method should reproduce the same ordering if the study is repeated. We
 287 approximate this stability using bootstrapping, which provides an estimate of the variability in the
 288 rankings. Details on the bootstrapping are described in Section F. Note that the WD and HiFiC
 289 studies employed active selection of comparison pairs. HiFiC used a binary search strategy, while
 290 WD selected pairs based on maximum information gain. For this reason, the bootstrapping results
 291 on these two datasets should be interpreted with caution.

292 We evaluate performance using two metrics. Top-1 agreement is the fraction of bootstrapped sam-
 293 ples that identify the same best item as the full dataset. Kendall’s Tau (τ) measures ordinal corre-
 294 lation between rankings (Kendall, 1938), with higher values indicating stable results. Top-1 agreement
 295 is most relevant when the best model matters, while Kendall’s Tau assesses overall ranking stability.

297 4.1 PERFORMANCE ACROSS DATASETS

298 We compare models across datasets to assess their performance on ranking accuracy and stability.
 299 Top-1 agreement and Kendall’s Tau are summarized in Table 1. Datasets with more comparisons per
 300 model, such as MT-Bench, WD, and HiFiC, are generally easier. Interestingly, HUMAINE deviates
 301 from this trend, highlighting that factors beyond the total number of comparisons, such as rater
 302 consistency and diversity, can influence model performance.

304 Overall, BBQ demonstrates superior stability and robustness across datasets. It identifies the top-
 305 performing item most frequently, being the shared best on three datasets. It recovers the overall
 306 ranking most accurately on five out of eight datasets, ranking second on the remaining three.

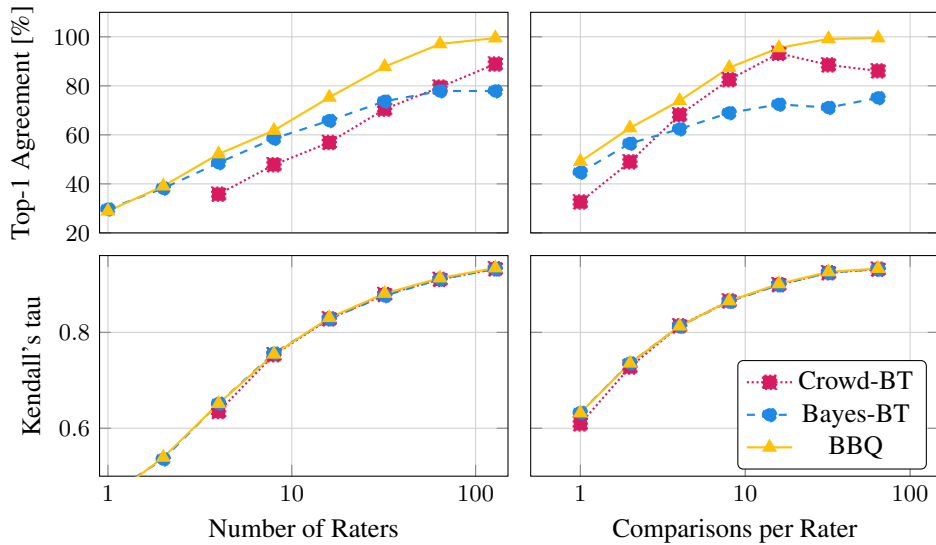
307 The three datasets where BBQ ranks second in Kendall’s Tau consist of high quality, homogeneous
 308 rater sets. On MT-Bench, all models perfectly recover the top item. The WD dataset, collected
 309 by Ballé et al. (2025), includes only five raters, likely the paper’s authors, suggesting exceptionally
 310 careful evaluation. In IHQ-screened, raters were explicitly filtered for quality. In such settings where
 311 rater quality is consistently high, explicitly modeling rater reliability offers little advantage, and the
 312 benefits of BBQ over simpler models are reduced.

313 Experiments on the IHQ dataset, considering both screened and unscreened rater subsets, reveal
 314 a clear pattern. BBQ substantially outperforms Crowd-BT and Bayes-BT when low-quality raters
 315 are present, as in CLIC-all and CLIC-unscreened. All three models achieve their best Top-1 accu-
 316 racy when restricted to the screened subset, highlighting the importance of rater selection. While
 317 Crowd-BT explicitly models rater quality, its performance drops noticeably on the full dataset, likely
 318 because crowdsourced raters provide fewer than 40 comparisons each, which increases susceptibil-
 319 ity to noisy annotations. In contrast, BBQ maintains strong performance even without screening,
 320 with only a minor decrease in Top-1 accuracy, demonstrating robustness to low-quality raters.

321 Nonetheless, achieving uniformly high rater quality is challenging. Large-scale crowdsourcing in-
 322 troduces variability, screening procedures are costly, and subjective factors may affect even diligent
 323 annotators. In this context, BBQ provides a principled way to leverage partially reliable raters while
 reducing the impact of noisy contributions.

324
 325 Table 1: Performance of different BT-based aggregation methods across several datasets. Top: Top-
 326 1 agreement [%], Bottom: Kendall’s Tau. BBQ most frequently identifies the top-performing item
 327 across all datasets, recovers the best overall ranking for more than half of the datasets, and ranks
 328 second on the remaining datasets.

	HUMAINE	MT-Bench	WD	HiFiC	ConHa	IHQ							
						all	scr.	unscr.					
Top-1 Agreement [%]													
Kendall’s Tau													
Crowd-BT	85.60	100.00	99.29	98.63	66.59	85.31	98.57	33.15					
Bayes-BT	97.30	100.00	100.00	100.00	57.30	75.07	98.90	24.32					
BBQ (ours)	97.50	100.00	100.00	100.00	77.12	99.32	99.80	61.92					



399 Figure 1: Scaling behavior of Bradley–Terry variants (Crowd-BT (Caron & Doucet, 2012), Bayes-
 400 BT (Chen et al., 2013), BBQ (ours)) on the IHQ-all dataset. **Left:** Performance vs. number of raters.
 401 **Right:** Performance vs. number of comparisons per rater. Both Top-1 agreement and Kendall’s τ
 402 improve noticeably with more raters or comparisons. While Top-1 agreement differentiates between
 403 models, Kendall’s τ remains similar across models. Crowd-BT fails to converge with very few
 404 raters, highlighting the EM algorithm’s advantage. Crowd-BT and BBQ perform similarly under
 405 sparse data, but BBQ outperforms Bayes-BT as the number of raters or comparisons grows.

367 4.2 SCALING WITH RATERS AND COMPARISONS

369 As observed in Table 1, datasets with more comparisons per model generally yield better performance.
 370 The number of comparisons can be increased in two ways: by adding more raters, or by
 371 increasing the number of comparisons each rater performs.

372 Figure 1 illustrates the impact of both factors on the three BT variants. The left column shows per-
 373 formance as a function of the number of raters (with the number of comparisons per rater fixed at the
 374 maximum), while the right column shows performance as a function of the number of comparisons
 375 per rater (with the number of raters fixed at the maximum). A clear difference in performance can
 376 be observed in Top-1 accuracy, while Kendall’s τ remains similar across models. Crowd-BT fails to
 377 converge with only one or two raters, highlighting the advantage of using the EM algorithm, which
 provides convergence guarantees compared to gradient descent.

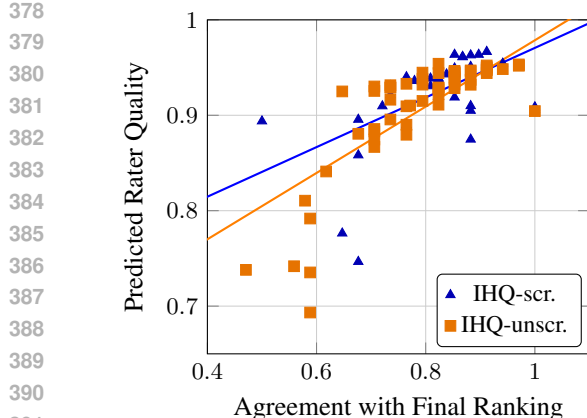


Figure 2: Scatter plot of rater agreement with the final ranking (x-axis) versus the predicted rater quality (y-axis) for the IHQ datasets. Each point corresponds to an individual rater. Triangles denote the filtered dataset, and squares denote the unfiltered dataset.

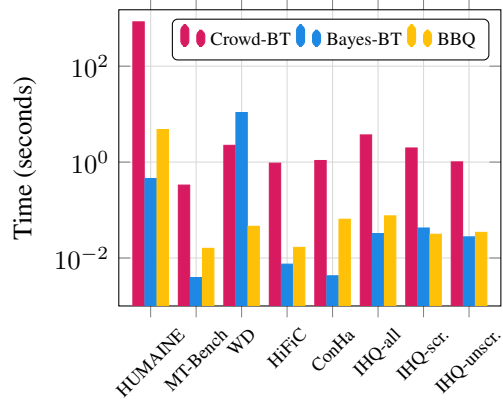


Figure 3: Average computation time in seconds (log-scale) for three models measured on a single bootstrapped sample across eight datasets. While Crowd-BT can require substantial computation time on some datasets, BBQ consistently remains fast across all datasets.

Crowd-BT and BBQ perform similarly when the number of raters or comparisons per rater is small. BBQ requires both multiple raters and multiple comparisons per rater to effectively distinguish between rater qualities. As the number of raters or comparisons per rater increases, BBQ increasingly outperforms Bayes-BT. In contrast, Bayes-BT tends to underperform overall but can surpass Crowd-BT when limited data per rater or a few number of raters are available, since Crowd-BT cannot reliably estimate rater quality in such sparse settings.

4.3 RATER QUALITY

Figure 2 shows the relationship between agreement with the final ranking and predicted rater quality. We observe a clear positive correlation: raters who agree more closely with the consensus ranking are assigned higher quality by the model. For the filtered dataset, the Pearson correlation is $r = 0.551$ across 50 raters. For the unfiltered dataset, the correlation is stronger, with $r = 0.724$ across 62 raters.

As expected, the unscreened dataset contains several raters with both lower agreement and lower predicted quality. Some raters in the IHQ-unscreened dataset even fall below the level of random guessing (50% agreement), systematically disagreeing with the majority. This highlights the importance of modeling rater quality when aggregating pairwise comparison data. BBQ successfully identifies such raters and assigns them lower quality scores, thereby reducing their influence on the final ranking and mitigating the noise they introduce.

4.4 COMPUTATIONAL EFFICIENCY

Figure 3 reports the average computation time in seconds required by each method to process a single bootstrapped sample across different datasets. These timings provide a practical perspective on the feasibility of the methods in real-world evaluation scenarios. BBQ consistently converges within a few seconds on all datasets. Crowd-BT requires more time than BBQ across the board, with particularly long runtimes on datasets with many comparisons, such as HUMAINE, where convergence takes around 15 minutes. Bayes-BT converges slowly on the WD dataset, though on other datasets it is slightly faster than BBQ. The efficiency of BBQ stems from the closed-form EM updates derived in our method, which enable rapid convergence even on large datasets.

It is also important to note that Crowd-BT was highly optimized and implemented in C (Kernighan & Ritchie, 1988), whereas BBQ was implemented using plain NumPy without specific optimizations. This suggests that BBQ could be made even faster with a compiled or vectorized implementation.

432 Consequently, BBQ is not only more robust and stable but also highly practical for large-scale human
 433 preference studies or applications that require repeated bootstrapping. The combination of accuracy,
 434 stability, and speed makes BBQ a compelling choice for real-world deployments.
 435

436 4.5 CONFIDENCE INTERVALS

437 We evaluate how Crowd-BT, Bayes-BT, and BBQ estimate uncertainty in item rankings. In a con-
 438 trolled simulation, raters provide pairwise comparisons of equally skilled items (H_0). Each model
 439 estimates skills and constructs uncertainty intervals to test for significant differences (Section G).
 440 The resulting Type I error rates are shown in Figure 6. At the 99% confidence level, the expected
 441 error rate is 1%. Crowd-BT and BBQ align closely, yielding slightly lower rates, while Bayes-
 442 BT is more conservative at $\sim 0.1\%$. Thus, Crowd-BT and BBQ provide well-calibrated uncertainty
 443 estimates, whereas Bayes-BT underestimates false positives.
 444

445 5 LIMITATIONS

446 Although BBQ effectively models rater quality, its advantages diminish in settings where all raters
 447 are uniformly reliable. In such homogeneous datasets, modeling variability provides little additional
 448 benefit. Ensuring consistently high-quality raters, however, often requires substantial cost and effort,
 449 which may not be feasible in large-scale studies. This tension highlights that BBQ is most useful in
 450 realistic crowdsourced settings, but less so when evaluations are carefully curated.
 451

452 Another limitation concerns the type of data the framework can handle. BBQ is currently restricted
 453 to pairwise comparisons, whereas many human evaluation studies use ratings, rankings, or multi-
 454 way inputs. Extending the model to handle these forms of feedback would broaden its applicability.
 455

456 From a methodological perspective, our experiments rely on a limited number of bootstrapped com-
 457 parisons. While this provides a practical measure of stability, larger-scale studies would be needed to
 458 further validate robustness. Additionally, the model assumes independence across comparisons and
 459 does not account for contextual or order effects, which may influence human judgments in practice.
 460

461 Finally, although BBQ scales well computationally, extremely large numbers of items or raters could
 462 still pose challenges without optimized or compiled implementations.
 463

464 6 CONCLUSION

465 We introduced BBQ, a Bayesian Bradley-Terry model that jointly estimates item quality and rater
 466 reliability. Our core contribution is the derivation of an Expectation-Maximization (EM) algorithm
 467 that simultaneously estimates item skills and individual rater quality, effectively down-weighting or
 468 removing the influence of unreliable participants. By explicitly modeling rater quality, the method
 469 produces more stable and accurate rankings. The EM algorithm ensures rapid convergence and
 470 monotonic likelihood improvement, addressing limitations of gradient-based approaches.
 471

472 Across diverse datasets, BBQ consistently achieved high Top-1 agreement and superior Kendall’s
 473 Tau, demonstrating both robustness and reliability. The model excels in scenarios with noisy or
 474 crowdsourced raters, maintaining accuracy even when raters contribute few comparisons. BBQ is
 475 particularly effective in large-scale settings where many raters are non-experts or vary widely in at-
 476 tentiveness and diligence. Our results highlight that incorporating rater quality is especially crucial
 477 when evaluation quality is heterogeneous or partially unreliable. Additionally, the Bayesian frame-
 478 work provides principled uncertainty estimates for item scores, enabling interpretable comparisons
 479 across studies. We further demonstrate that the model’s error bars are well-calibrated and can be
 480 used to assess whether differences between items are statistically significant. Predicted rater quality
 481 aligns with agreement to final rankings, validating the model’s ability to identify reliable evaluators.
 482

483 Overall, BBQ advances human evaluation methodology by offering a practical, interpretable, and
 484 generalizable approach to aggregate noisy pairwise comparisons. This work contributes a significant
 485 step toward more cost-effective, interpretable, and reproducible human studies for evaluating AI-
 486 generated content.
 487

486 REPRODUCIBILITY STATEMENT
487

488 The code used in our experiments is provided in the supplementary material, along with a detailed
489 README that explains how to set up the environment and run all bootstrapping experiments. The
490 supplementary material also includes all datasets used in our study, including the publicly available
491 datasets on which we ran our experiments. In addition, our newly collected dataset is included,
492 making it fully accessible for replication and further research. For the camera-ready version, we will
493 make both the code and all datasets publicly available. We also provide comprehensive descriptions
494 of the proposed model (Section 3), experimental setup (Section 4), hyperparameters (Section C),
495 and data collection procedures (Section E).

496 REFERENCES
497

498 Till Aczel and Roger Wattenhofer. Conditional hallucinations for image compression. *arXiv preprint*
499 *arXiv:2410.19493*, 2024.

500 Eldridge S Adams. Bayesian analysis of linear dominance hierarchies. *Animal Behaviour*, 69(5):
501 1191–1201, 2005.

502 Alan Agresti. *Analysis of ordinal categorical data*. John Wiley & Sons, 2010.

503 Jona Ballé, Luca Versari, Emilien Dupont, Hyunjik Kim, and Matthias Bauer. Good, cheap, and
504 fast: Overfitted image compression with wasserstein distortion. In *Proceedings of the Computer*
505 *Vision and Pattern Recognition Conference*, pp. 23259–23268, 2025.

506 Ralph Allan Bradley and Milton E Terry. Rank analysis of incomplete block designs: I. the method
507 of paired comparisons. *Biometrika*, 39(3/4):324–345, 1952.

508 Francois Caron and Arnaud Doucet. Efficient bayesian inference for generalized bradley–terry mod-
509 els. *Journal of Computational and Graphical Statistics*, 21(1):174–196, 2012.

510 Xi Chen, Paul N Bennett, Kevyn Collins-Thompson, and Eric Horvitz. Pairwise ranking aggregation
511 in a crowdsourced setting. In *Proceedings of the sixth ACM international conference on Web*
512 *search and data mining*, pp. 193–202, 2013.

513 Wei-Lin Chiang, Lianmin Zheng, Ying Sheng, Anastasios Nikolas Angelopoulos, Tianle Li,
514 Dacheng Li, Banghua Zhu, Hao Zhang, Michael Jordan, Joseph E Gonzalez, et al. Chatbot
515 arena: An open platform for evaluating llms by human preference. In *Forty-first International*
516 *Conference on Machine Learning*, 2024.

517 CLIC. Clic 2024: Challenge on learned image compression. [https://archive.](https://archive.compression.cc/2024/)
518 [compression.cc/2024/](https://archive.compression.cc/2024/), 2025. Accessed: 2025-09-12.

519 Arthur P Dempster, Nan M Laird, and Donald B Rubin. Maximum likelihood from incomplete data
520 via the em algorithm. *Journal of the royal statistical society: series B (methodological)*, 39(1):
521 1–22, 1977.

522 Persi Diaconis. Group representations in probability and statistics. *Lecture notes-monograph series*,
523 11:i–192, 1988.

524 Lester R Ford Jr. Solution of a ranking problem from binary comparisons. *The American Mathe-
525 matical Monthly*, 64(8P2):28–33, 1957.

526 Rafael C Gonzalez. *Digital image processing*. Pearson education india, 2009.

527 Google. Google, 2025. URL [https://github.com/google-research/](https://github.com/google-research/google-research)
528 [google-research](https://github.com/google-research). Accessed: 2025-09-12.

529 John Guiver and Edward Snelson. Bayesian inference for plackett-luce ranking models. In *proceed-
530 ings of the 26th annual international conference on machine learning*, pp. 377–384, 2009.

531 Martin Heusel, Hubert Ramsauer, Thomas Unterthiner, Bernhard Nessler, and Sepp Hochreiter.
532 Gans trained by a two time-scale update rule converge to a local nash equilibrium. *Advances in*
533 *neural information processing systems*, 30, 2017.

540 Tzu-Kuo Huang, Ruby C Weng, Chih-Jen Lin, and Greg Ridgeway. Generalized bradley-terry
 541 models and multi-class probability estimates. *Journal of Machine Learning Research*, 7(1), 2006.
 542

543 David R Hunter. Mm algorithms for generalized bradley-terry models. *The annals of statistics*, 32
 544 (1):384–406, 2004.

545 Frederick Jelinek. *Statistical methods for speech recognition*. MIT press, 1998.
 546

547 Maurice G Kendall. A new measure of rank correlation. *Biometrika*, 30(1-2):81–93, 1938.
 548

549 Brian W. Kernighan and Dennis M. Ritchie. *The C Programming Language*. Prentice Hall, 1988.

550 Kenneth Lange, David R Hunter, and Ilsoon Yang. Optimization transfer using surrogate objective
 551 functions. *Journal of computational and graphical statistics*, 9(1):1–20, 2000.
 552

553 Mabyduck Ltd. Mabyduck, 2025. URL <https://www.mabyduck.com/>. Accessed: 2025-09-
 554 12.

555 R Duncan Luce et al. *Individual choice behavior*, volume 4. Wiley New York, 1959.
 556

557 Fabian Mentzer, George D Toderici, Michael Tschannen, and Eirikur Agustsson. High-fidelity generative
 558 image compression. *Advances in neural information processing systems*, 33:11913–11924,
 559 2020.

560 Kishore Papineni, Salim Roukos, Todd Ward, and Wei-Jing Zhu. Bleu: a method for automatic
 561 evaluation of machine translation. In *Proceedings of the 40th annual meeting of the Association
 562 for Computational Linguistics*, pp. 311–318, 2002.

563 Robin L Plackett. The analysis of permutations. *Journal of the Royal Statistical Society Series C:
 564 Applied Statistics*, 24(2):193–202, 1975.
 565

566 Pejaver V Rao and Lawrence L Kupper. Ties in paired-comparison experiments: A generalization
 567 of the bradley-terry model. *Journal of the American Statistical Association*, 62(317):194–204,
 568 1967.

569 Prolific AI Team. Humaine: Human-ai interaction evaluation dataset, 2025. URL <https://huggingface.co/datasets/ProlificAI/humaine-evaluation-dataset>.
 570

571 Kexin Wang, Yunlong Zhao, Qianqian Dong, Tom Ko, and Mingxuan Wang. Mospc: Mos prediction
 572 based on pairwise comparison. *arXiv preprint arXiv:2306.10493*, 2023.

573 Zhou Wang, Eero P Simoncelli, and Alan C Bovik. Multiscale structural similarity for image quality
 574 assessment. In *The thirty-seventh asilomar conference on signals, systems & computers, 2003*,
 575 volume 2, pp. 1398–1402. Ieee, 2003.
 576

577 Emin Zerman, Vedad Hulusic, Giuseppe Valenzise, Rafał K Mantiuk, and Frédéric Dufaux. The
 578 relation between mos and pairwise comparisons and the importance of cross-content comparisons.
 579 *Electronic Imaging*, 30:1–6, 2018.
 580

581 Ernst Zermelo. Die berechnung der turnier-ergebnisse als ein maximumproblem der wahrschein-
 582 lichkeitsrechnung. *Mathematische Zeitschrift*, 29(1):436–460, 1929.
 583

584 Lianmin Zheng, Wei-Lin Chiang, Ying Sheng, Siyuan Zhuang, Zhanghao Wu, Yonghao Zhuang,
 585 Zi Lin, Zhuohan Li, Dacheng Li, Eric. P Xing, Hao Zhang, Joseph E. Gonzalez, and Ion Stoica.
 586 Judging Ilm-as-a-judge with mt-bench and chatbot arena, 2023.
 587

588

589

590

591

592

593

594 **A USAGE OF LLMs**
 595

596 During the preparation of this paper, we utilized large language models (LLMs) as supportive tools.
 597 ChatGPT, Claude, Gemini, and Grammarly assisted with spellchecking, refining phrasing, and con-
 598 densing text to enhance clarity and readability. Additionally, ChatGPT, Claude, and Cursor were
 599 used for code analysis, completion, and the generation of visualizations to aid our development
 600 workflow. These tools were employed solely as auxiliary aids, while all core research ideas, experi-
 601 mental design, and interpretation of results were developed independently by the authors.
 602

603 **B BAYESIAN BT WITH RATER QUALITY DERIVATION**
 604

605 We consider R raters comparing K items. Each rater r has quality q_r , meaning that with probability
 606 q_r they follow the Bradley–Terry model, and with probability $1 - q_r$ they choose randomly. The
 607 following is a standard EM (Dempster et al., 1977) derivation that incorporates these rater-specific
 608 reliabilities into the Bayesian estimation framework.
 609

610 **B.1 MODEL DEFINITION**
 611

612 Notation:

- 614 • $\lambda = (\lambda_1, \dots, \lambda_K)$: skill parameters for the K items.
- 615 • $q = (q_1, \dots, q_R)$: quality parameters for the R raters.
- 616 • $Y_i \sim \mathcal{E}(\lambda_i)$: latent arrival time associated with item i .
- 617 • $A_{r,ij}^{(c)} \sim \text{Bernoulli}(q_r)$: indicator that the c -th comparison of pair (i, j) by rater r follows
 618 the Bradley–Terry model.
- 619 • $n_{r,ij}$: total number of comparisons of (i, j) by rater r .
- 620 • $n_{ij} = \sum_{r=1}^R n_{r,ij}$: total number of comparisons of (i, j) .
- 621 • $w_{r,ij}$: number of times rater r ranked i above j .
- 622 • $w_{ij} = \sum_{r=1}^R w_{r,ij}$: total number of times i was ranked above j .
- 623 • $m_{r,ij} = \sum_{c=1}^{n_{r,ij}} A_{r,ij}^{(c)}$: number of Bradley–Terry-model comparisons of (i, j) by rater r .
- 624 • $m_{ij} = \sum_{r=1}^R m_{r,ij}$: total number of Bradley–Terry-model comparisons of (i, j) .
- 625 • $v_{r,ij} = \sum_{c=1}^{w_{r,ij}} A_{r,ij}^{(c)}$: number of Bradley–Terry-model wins of i over j by rater r .
- 626 • $v_{ij} = \sum_{r=1}^R v_{r,ij}$: total number of Bradley–Terry-model wins of i over j .
- 627 • $Z_{r,ij} = \sum_{c=1}^{n_{r,ij}} A_{r,ij}^{(c)} \min(Y_i^{(c)}, Y_j^{(c)})$: sum of minimal arrival times, with
 628
- 629
- 630
- 631
- 632
- 633
- 634
- 635
- 636
- 637

$$Z_{r,ij} \mid m_{r,ij} \sim \Gamma(m_{r,ij}, \lambda_i + \lambda_j).$$

Bradley–Terry probability:

$$P(i \text{ beats } j) = \frac{\lambda_i}{\lambda_i + \lambda_j}.$$

Mixture with rater quality:

$$P(r \text{ ranks } i \text{ above } j) = q_r \frac{\lambda_i}{\lambda_i + \lambda_j} + (1 - q_r) \frac{1}{2}.$$

Latent exponential view:

$$Y_i \sim \mathcal{E}(\lambda_i), \quad Y_j \sim \mathcal{E}(\lambda_j), \quad P(i \text{ beats } j) = P(Y_i < Y_j).$$

648 B.2 COMPLETE-DATA LOG-LIKELIHOOD
649

650

651 We need to compute:
652

653

654

655
$$\ell_c(\lambda, q; D, Z, A) = \log P(D, Z, A | \lambda, q)$$

656
$$= \log P(Z | D, A, \lambda, q) + \log P(A | D, \lambda, q) + \log P(D | \lambda, q)$$

657

658

659

660

661 Log-Likelihood of $P(Z | A, \lambda)$:
662

663

664

665
$$\log P(Z | D, A, \lambda, q) = \sum_{i=1}^K \sum_{j=i+1}^K \left[m_{ij} \log(\lambda_i + \lambda_j) - (\lambda_i + \lambda_j) z_{ij} \right. \\ 666 \left. + (m_{ij} - 1) \log z_{ij} - \log \Gamma(m_{ij}) \right]$$

667

668

669

670

671

672

673 Log-Likelihood of $P(A | q)$:
674

675

676

677
$$\log P(A | D, \lambda, q) = \sum_{r=1}^R \sum_{i=1}^K \sum_{j=i+1}^K \left[m_{r,ij} \log q_r + (n_{r,ij} - m_{r,ij}) \log(1 - q_r) \right]$$

678

679

680

681

682

683 Log-Likelihood of $P(D | \lambda, A)$:
684

685

686

687
$$\log P(D | \lambda, q) = \sum_{r=1}^R \sum_{i=1}^K \sum_{\substack{j=1 \\ j \neq i}}^K \left[v_{r,ij} \log \frac{\lambda_i}{\lambda_i + \lambda_j} + (w_{r,ij} - v_{r,ij}) \log \frac{1}{2} \right]$$

688

689

690

691
$$= \sum_{r=1}^R \sum_{i=1}^K [v_{ir} \log \lambda_i] \\ 692 \quad - \sum_{r=1}^R \sum_{i=1}^K \sum_{j=i+1}^K [(v_{r,ij} + v_{r,ji}) \log (\lambda_i + \lambda_j) + (w_{r,ij} + w_{r,ji} - v_{r,ij} - v_{r,ji}) \log 2] \\ 693 \\ 694 \\ 695 \\ 696 \\ 697 \\ 698 \\ 699 \\ 700 \\ 701$$

$$= \sum_{i=1}^K [v_i \log \lambda_i] \\ - \sum_{i=1}^K \sum_{j=i+1}^K [m_{ij} \log (\lambda_i + \lambda_j) + (n_{ij} - m_{ij}) \log 2]$$

702 Complete-Data Log-Likelihood:
 703 $\ell_c(\lambda, q; D, Z, A) = \log P(Z | D, A, \lambda, q) + \log P(A | D, \lambda, q) + \log P(D | \lambda, q)$
 704 $= \sum_{i=1}^K \sum_{j=i+1}^K \left[m_{ij} \log(\lambda_i + \lambda_j) - (\lambda_i + \lambda_j) z_{ij} + (m_{ij} - 1) \log z_{ij} - \log \Gamma(m_{ij}) \right]$
 705 $+ \sum_{r=1}^R \sum_{i=1}^K \sum_{j=i+1}^K \left[m_{r,ij} \log q_r + (n_{r,ij} - m_{r,ij}) \log(1 - q_r) \right]$
 706 $+ \sum_{i=1}^K [v_i \log \lambda_i]$
 707 $- \sum_{i=1}^K \sum_{j=i+1}^K [m_{ij} \log (\lambda_i + \lambda_j) + (n_{ij} - m_{ij}) \log 2]$
 708 $= \sum_{i=1}^K \sum_{j=i+1}^K \left[(n_{ij} - m_{ij}) \log 2 - (\lambda_i + \lambda_j) z_{ij} + (m_{ij} - 1) \log z_{ij} - \log \Gamma(m_{ij}) \right]$
 709 $+ \sum_{r=1}^R \sum_{i=1}^K \sum_{j=i+1}^K \left[m_{r,ij} \log q_r + (n_{r,ij} - m_{r,ij}) \log(1 - q_r) \right]$
 710 $+ \sum_{i=1}^K [v_i \log \lambda_i]$
 711

726 B.3 EXPECTATION STEP

727 We introduce conjugate priors: Gamma distribution $\lambda_i \sim \Gamma(a, b)$ for each item i , and Beta $q_r \sim$
 728 $B(\alpha, \beta)$ for each rater r .

729 The Q -function is the expectation of the complete-data log-posterior:
 730

$$731 Q(\lambda, q | \lambda^*, q^*) = \mathbb{E}_{A, Z | D, \lambda^*, q^*} [\ell_c(\lambda, q; D, Z, A) + \log P(\lambda) + \log P(q)].$$

732 Posterior probability of a Bradley-Terry-consistent annotation:
 733

$$734 P(A_{r,ij}^{(k)} = 1 | i \succ j) = \frac{P(i \succ j | A = 1) P(A = 1)}{P(i \succ j | A = 1) P(A = 1) + P(i \succ j | A = 0) P(A = 0)} \\ 735 = \frac{\left(\frac{\lambda_i^*}{\lambda_i^* + \lambda_j^*} \right) q_r^*}{\left(\frac{\lambda_i^*}{\lambda_i^* + \lambda_j^*} \right) q_r^* + \frac{1}{2} (1 - q_r^*)} = \gamma_{r,ij}^*.$$

736 Expected sufficient statistics:
 737

$$738 \mathbb{E}[m_{r,ij}] = w_{r,ij} \gamma_{r,ij}^* + w_{r,ji} \gamma_{r,ji}^* \\ 739 \mathbb{E}[m_{ij}] = \sum_{r=1}^R (w_{r,ij} \gamma_{r,ij}^* + w_{r,ji} \gamma_{r,ji}^*) \\ 740 \mathbb{E}[v_{r,ij}] = w_{r,ij} \gamma_{r,ij}^* \\ 741 \mathbb{E}[v_{ir}] = \sum_{j:j \neq i}^K w_{r,ij} \gamma_{r,ij}^* \\ 742 \mathbb{E}[v_i] = \sum_{r=1}^R \sum_{j:j \neq i}^K w_{r,ij} \gamma_{r,ij}^* \\ 743 \mathbb{E}[z_{ij}] = \frac{\sum_{r=1}^R (w_{r,ij} \gamma_{r,ij}^* + w_{r,ji} \gamma_{r,ji}^*)}{\lambda_i^* + \lambda_j^*}.$$

756 Expected complete-data log-posterior:
 757

$$\begin{aligned}
 758 \quad \mathbb{E}[\ell_c] &= \sum_{i=1}^K \sum_{j=i+1}^K \left[-(\lambda_i + \lambda_j) \frac{\sum_{r=1}^R (w_{r,ij}\gamma_{r,ij}^* + w_{r,ji}\gamma_{r,ji}^*)}{\lambda_i^* + \lambda_j^*} \right] \\
 759 \\
 760 \quad &+ \sum_{r=1}^R \sum_{i=1}^K \sum_{j=i+1}^K \left[(w_{r,ij}\gamma_{r,ij}^* + w_{r,ji}\gamma_{r,ji}^*) \log q_r \right. \\
 761 \\
 762 \quad &\quad \left. + (n_{r,ij} - (w_{r,ij}\gamma_{r,ij}^* + w_{r,ji}\gamma_{r,ji}^*)) \log(1 - q_r) \right] \\
 763 \\
 764 \quad &+ \sum_{i=1}^K \sum_{\substack{j=1 \\ j \neq i}}^K w_{r,ij}\gamma_{r,ij}^* \log \lambda_i \\
 765 \\
 766 \quad &+ \text{const.}
 \end{aligned}$$

771 Priors contribute:
 772

$$\begin{aligned}
 773 \quad \mathbb{E}[\log P(\lambda)] &= \sum_{i=1}^K [(a - 1) \log \lambda_i - b \lambda_i], \\
 774 \\
 775 \quad \mathbb{E}[\log P(q)] &= \sum_{r=1}^R [(\alpha - 1) \log q_r + (\beta - 1) \log(1 - q_r)].
 \end{aligned}$$

779 Final Q -function:
 780

$$\begin{aligned}
 781 \quad Q(\lambda, q \mid \lambda^*, q^*) &= \sum_{i=1}^K \sum_{j=i+1}^K \left[-(\lambda_i + \lambda_j) \frac{\sum_{r=1}^R (w_{r,ij}\gamma_{r,ij}^* + w_{r,ji}\gamma_{r,ji}^*)}{\lambda_i^* + \lambda_j^*} \right] \\
 782 \\
 783 \quad &+ \sum_{r=1}^R \sum_{i=1}^K \sum_{j=i+1}^K \left[(w_{r,ij}\gamma_{r,ij}^* + w_{r,ji}\gamma_{r,ji}^*) \log q_r \right. \\
 784 \\
 785 \quad &\quad \left. + (n_{r,ij} - (w_{r,ij}\gamma_{r,ij}^* + w_{r,ji}\gamma_{r,ji}^*)) \log(1 - q_r) \right] \\
 786 \\
 787 \quad &+ \sum_{i=1}^K \sum_{\substack{j=1 \\ j \neq i}}^K w_{r,ij}\gamma_{r,ij}^* \log \lambda_i \\
 788 \\
 789 \quad &+ \sum_{i=1}^K [(a - 1) \log \lambda_i - b \lambda_i] \\
 790 \\
 791 \quad &+ \sum_{r=1}^R [(\alpha - 1) \log q_r + (\beta - 1) \log(1 - q_r)] \\
 792 \\
 793 \quad &+ \text{const.}
 \end{aligned}$$

800 where
 801

$$\gamma_{r,ij}^* = \frac{q_r^* \frac{\lambda_i^*}{\lambda_i^* + \lambda_j^*}}{q_r^* \frac{\lambda_i^*}{\lambda_i^* + \lambda_j^*} + (1 - q_r^*)^{\frac{1}{2}}}.$$

806 B.4 M-STEP

807 The M-step maximizes the Q -function w.r.t. the parameters (λ, q) , holding the expectations com-
 808 puted in the E-step fixed.
 809

810 **Update for q_r** The update for each rater quality q_r is obtained by maximizing Q with respect to
 811 q_r (including the Beta prior).

$$\begin{aligned}
 816 \quad Q(q | \lambda^*, q^*) &= \sum_{r=1}^R \sum_{i=1}^K \sum_{j=i+1}^K \left[(w_{r,ij}\gamma_{r,ij}^* + w_{r,ji}\gamma_{r,ji}^*) \log q_r \right. \\
 817 &\quad \left. + (n_{r,ij} - (w_{r,ij}\gamma_{r,ij}^* + w_{r,ji}\gamma_{r,ji}^*)) \log(1 - q_r) \right] \\
 818 &\quad + (\alpha - 1) \log q_r + (\beta - 1) \log(1 - q_r) + \text{const.} \\
 819 \quad \frac{\partial Q}{\partial q_r} &= \sum_{i=1}^K \sum_{j=i+1}^K \left[\frac{w_{r,ij}\gamma_{r,ij}^* + w_{r,ji}\gamma_{r,ji}^*}{q_r} - \frac{n_{r,ij} - (w_{r,ij}\gamma_{r,ij}^* + w_{r,ji}\gamma_{r,ji}^*)}{1 - q_r} \right] \\
 820 &\quad + \frac{\alpha - 1}{q_r} - \frac{\beta - 1}{1 - q_r} \\
 821 \quad 0 &\stackrel{!}{=} \frac{\sum_{i=1}^K \sum_{j=i+1}^K (w_{r,ij}\gamma_{r,ij}^* + w_{r,ji}\gamma_{r,ji}^*) + (\alpha - 1)}{q_r} \\
 822 &\quad - \frac{\sum_{i=1}^K \sum_{j=i+1}^K (n_{r,ij} - (w_{r,ij}\gamma_{r,ij}^* + w_{r,ji}\gamma_{r,ji}^*)) + (\beta - 1)}{1 - q_r} \\
 823 &\implies (1 - q_r) \left(\sum_{i=1}^K \sum_{j=i+1}^K (w_{r,ij}\gamma_{r,ij}^* + w_{r,ji}\gamma_{r,ji}^*) + (\alpha - 1) \right) \\
 824 &\implies q_r \left(\sum_{i=1}^K \sum_{j=i+1}^K (n_{r,ij} - (w_{r,ij}\gamma_{r,ij}^* + w_{r,ji}\gamma_{r,ji}^*)) + (\beta - 1) \right) \\
 825 &\implies q_r = \frac{\sum_{i=1}^K \sum_{j=i+1}^K (w_{r,ij}\gamma_{r,ij}^* + w_{r,ji}\gamma_{r,ji}^*) + (\alpha - 1)}{\sum_{i=1}^K \sum_{j=i+1}^K (w_{r,ij}\gamma_{r,ij}^* + w_{r,ji}\gamma_{r,ji}^* + n_{r,ij} - (w_{r,ij}\gamma_{r,ij}^* + w_{r,ji}\gamma_{r,ji}^*)) + (\beta + \alpha - 2)} \\
 826 &\implies q_r^{(t)} = \frac{\sum_{i=1}^K \sum_{j=i+1}^K (w_{r,ij}\gamma_{r,ij}^{(t-1)} + w_{r,ji}\gamma_{r,ji}^{(t-1)}) + (\alpha - 1)}{n_r + \beta + \alpha - 2}
 \end{aligned}$$

845 where the last line gives the explicit update at iteration t .

850 **Update for λ_i** The update for each item skill λ_i is obtained by maximizing Q with respect to λ_i
 851 (including the Gamma prior).

$$\begin{aligned}
 855 \quad Q(\lambda | \lambda^*, q^*) &= \sum_{i=1}^K \sum_{j=i+1}^K -(\lambda_i + \lambda_j) \frac{\sum_{r=1}^R (w_{r,ij}\gamma_{r,ij}^* + w_{r,ji}\gamma_{r,ji}^*)}{\lambda_i^* + \lambda_j^*} \\
 856 &\quad + \sum_{r=1}^R \sum_{i=1}^K \sum_{\substack{j=1 \\ j \neq i}}^K w_{r,ij}\gamma_{r,ij}^* \log \lambda_i \\
 857 &\quad + \sum_{i=1}^K [(a - 1) \log \lambda_i - b\lambda_i] + \text{const.}
 \end{aligned}$$

$$\begin{aligned}
& \frac{\partial Q}{\partial \lambda_i} = - \sum_{j \neq i}^K \frac{\sum_{r=1}^R (w_{r,ij} \gamma_{r,ij}^* + w_{r,ji} \gamma_{r,ji}^*)}{\lambda_i^* + \lambda_j^*} + \sum_{r=1}^R \frac{\sum_{j \neq i}^K w_{r,ij} \gamma_{r,ij}^*}{\lambda_i} + \frac{a-1}{\lambda_i} - b \\
& 0 \stackrel{!}{=} \frac{\sum_{r=1}^R \sum_{j \neq i}^K w_{r,ij} \gamma_{r,ij}^* + (a-1)}{\lambda_i} - \sum_{j \neq i}^K \frac{\sum_{r=1}^R (w_{r,ij} \gamma_{r,ij}^* + w_{r,ji} \gamma_{r,ji}^*)}{\lambda_i^* + \lambda_j^*} - b \\
\implies \lambda_i^{(t)} &= \frac{\sum_{r=1}^R \sum_{j \neq i}^K w_{r,ij} \gamma_{r,ij}^{(t-1)} + (a-1)}{\sum_{j \neq i}^K \frac{\sum_{r=1}^R (w_{r,ij} \gamma_{r,ij}^{(t-1)} + w_{r,ji} \gamma_{r,ji}^{(t-1)})}{\lambda_i^{(t-1)} + \lambda_j^{(t-1)}} + b} \\
\gamma_{r,ij}^{(t-1)} &= \frac{q_r^{(t-1)} \frac{\lambda_i^{(t-1)}}{\lambda_i^{(t-1)} + \lambda_j^{(t-1)}}}{q_r^{(t-1)} \frac{\lambda_i^{(t-1)}}{\lambda_i^{(t-1)} + \lambda_j^{(t-1)}} + (1 - q_r^{(t-1)}) \frac{1}{2}}
\end{aligned}$$

where the last line gives the explicit update at iteration t .

C HYPERPARAMETERS

For Crowd-BT, we use the implementation of Google (2025) with the default hyperparameters.

The only hyperparameters in the Bayes-BT and BBQ models are the prior distribution parameters and the stopping thresholds. For both Bayes-BT and BBQ, we consider the model converged when no ELO score changes by more than 1 between two iterations. The ELO score can be calculated from the skill parameter λ as:

$$\text{ELO} = \log(\text{skill}) \cdot \text{ELO_SCALE_FACTOR}. \quad (14)$$

where we set the ELO_SCALE_FACTOR to 400.

We chose a gamma prior with shape 5 and rate 0.1 for the skill parameters in both Bayes-BT and BBQ. For BBQ, the beta prior on the rater quality has $\alpha = 10$ and $\beta = 2$.

D DATASETS

We evaluate our models on a diverse set of human preference datasets covering both language and image domains. Table 2 provides an overview.

For natural language, we use the HUMAINE dataset (Team, 2025), a large-scale benchmark with over 100k comparisons, and MT-Bench (Zheng et al., 2023), which provides model comparison judgments from crowd workers on multi-turn dialogues.

For image compression, we consider three datasets: WD (Ballé et al., 2025), a dense expert-labeled dataset with thousands of comparisons per rater; HiFiC (Mentzer et al., 2020), which evaluates learned image codecs; and ConHa (Aczel & Wattenhofer, 2024), which focuses on conditional generative models. These datasets vary substantially in scale, number of raters, and rater expertise, providing a broad testbed for robustness.

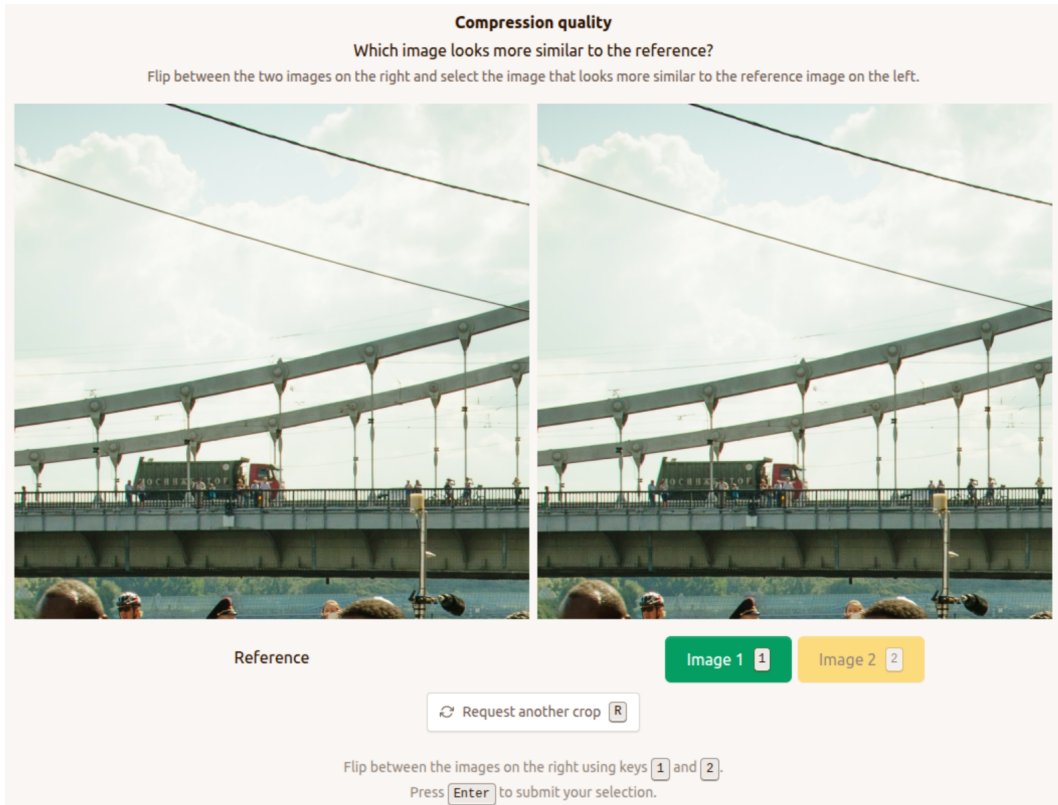
Finally, we introduce the inhomogeneous rater quality (**IHQ**) dataset, obtained from a user study on the CLIC2024 (CLIC, 2025) data conducted via the *Mabyduck* platform. It contains two-alternative-forced-choice (2AFC) judgments across 28 generative image compression models. To study the impact of rater quality, we provide two subsets: (i) **screened**, where raters passed pre-screening checks for attention and display quality, and (ii) **unscreened**, where all raters are included. The screened subset represents higher-quality raters, whereas the unscreened subset better reflects the noisy conditions typical of large-scale human evaluations.

This collection of datasets allows us to study both large-scale, relatively clean benchmarks and smaller, noisier settings where modeling rater reliability is critical.

918

919 Table 2: Summary of datasets used in our experiments. The IHQ dataset was collected by us on
 920 the Mabyduck platform and includes both 2AFC and 3AFC settings. For this dataset, we provide
 921 screened and unscreened subsets: screened subsets include only raters who passed pre-screening
 922 tests for attention and display quality, ensuring higher reliability, while unscreened subsets include
 923 all raters.

dataset	# comparisons	# raters	# models	comp/rater	comp/model
HUMAINE (Team, 2025)	105,220	1,977	27	53.2	3897.0
MT-Bench (Zheng et al., 2023)	3,355	65	6	51.6	559.2
WD (Ballé et al., 2025)	16,659	5	30	3331.8	555.3
HiFiC (Mentzer et al., 2020)	5,220	20	9	261.0	580.0
ConHa (Aczel & Wattenhofer, 2024)	1,531	40	8	38.3	191.4
IHQ-all	4,074	112	28	36.4	145.5
IHQ-screened	2,012	50	28	40.2	71.9
IHQ-unscreened	2,062	62	28	33.3	73.6



954

955 Figure 4: Screenshot of the Mabyduck user study platform used for collecting pairwise comparisons.
 956 A reference image is shown on the left, and the rater selects between two compressed images on the
 957 right.
 958

959

960 E USER STUDY PLATFORM

961

962

963 All pairwise comparisons on the CLIC2024 (CLIC, 2025) dataset were collected using the Maby-
 964 duck platform (Ltd., 2025). A screenshot of the platform can be seen in Figure 4. The task asks:
 965 “Which image looks more similar to the reference image?” Ties are not allowed, and all pairs were
 966 selected uniformly at random.

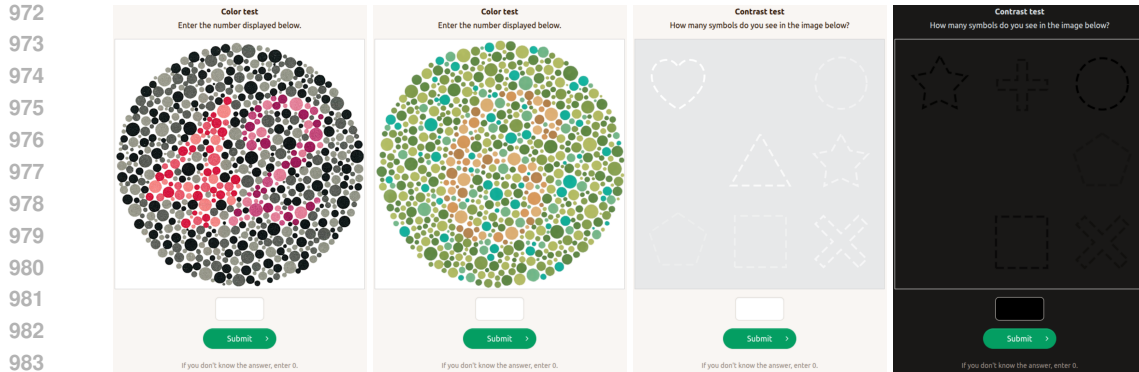


Figure 5: Four example images from the pre-screening process for raters. The first two are color blindness tests, where raters must identify the number displayed in each pattern. The last two are shape detection tests designed to evaluate sensitivity to low-contrast objects: one light gray shape on a white background and one dark gray shape on a black background.

To study rater quality, we split the IHQ dataset into screened and unscreened subsets. Screened raters passed pre-tests for color vision, display contrast, and sensitivity to subtle differences, and completed training comparisons choosing the higher-quality image to reinforce evaluation criteria.

Figure 5 shows four example images from the pre-screening process. The first two are standard color blindness tests, where raters must correctly identify the number shown in each pattern. The final two images are shape detection tests designed to evaluate the raters’ sensitivity to low-contrast objects: one features a light gray shape on a white background, and the other a dark gray shape on a black background. These pre-screening tests help ensure that only raters with adequate visual capabilities contribute to the screened subset.

F BOOTSTRAPPING DETAILS

Since both BBQ and Crowd-BT explicitly model rater quality, we perform bootstrapping over raters rather than individual comparisons. This approach preserves each rater’s comparison distribution and ensures a fair assessment of stability. For all datasets, we perform 10,000 bootstrap resamples of raters, except for the HUMAINE dataset, where a single bootstrap iteration for Crowd-BT takes approximately 15 minutes, as discussed in Section 4.4. On the HUMAINE dataset, we perform 1,000 resamples to reduce computation time.

G UNCERTAINTY ESTIMATION DETAILS

In addition to ranking items, estimating uncertainty is important to assess whether observed differences are statistically significant.

The Bayesian Bradley-Terry (Bayes-BT) and Bayesian Bradley-Terry with Quality (BBQ) models quantify uncertainty via the posterior distribution over item skills. Each skill has a Gamma prior, which is updated using the observed pairwise comparisons. Credible intervals derived from the posterior are then converted to the Elo scale to facilitate comparison across items.

The classical Crowd-BT model, being non-Bayesian, estimates uncertainty using a frequentist approximation. Specifically, a second-order Taylor expansion around the maximum likelihood estimate is employed. The Hessian of the log-likelihood is inverted to obtain the covariance matrix, whose diagonal entries correspond to the variances of individual items. These variances are converted to 99% confidence intervals via:

$$p_{99} = \sqrt{\text{diag}(\text{covariance})} \times k_{\text{Erfc}0.01} \times \sqrt{2} \approx \sqrt{\text{diag}(\text{covariance})} \times 3.29,$$

where the constants scale the standard deviation to match the 99% confidence level. Narrower likelihood peaks yield smaller intervals, reflecting higher certainty, while flatter peaks produce larger intervals, indicating greater uncertainty.

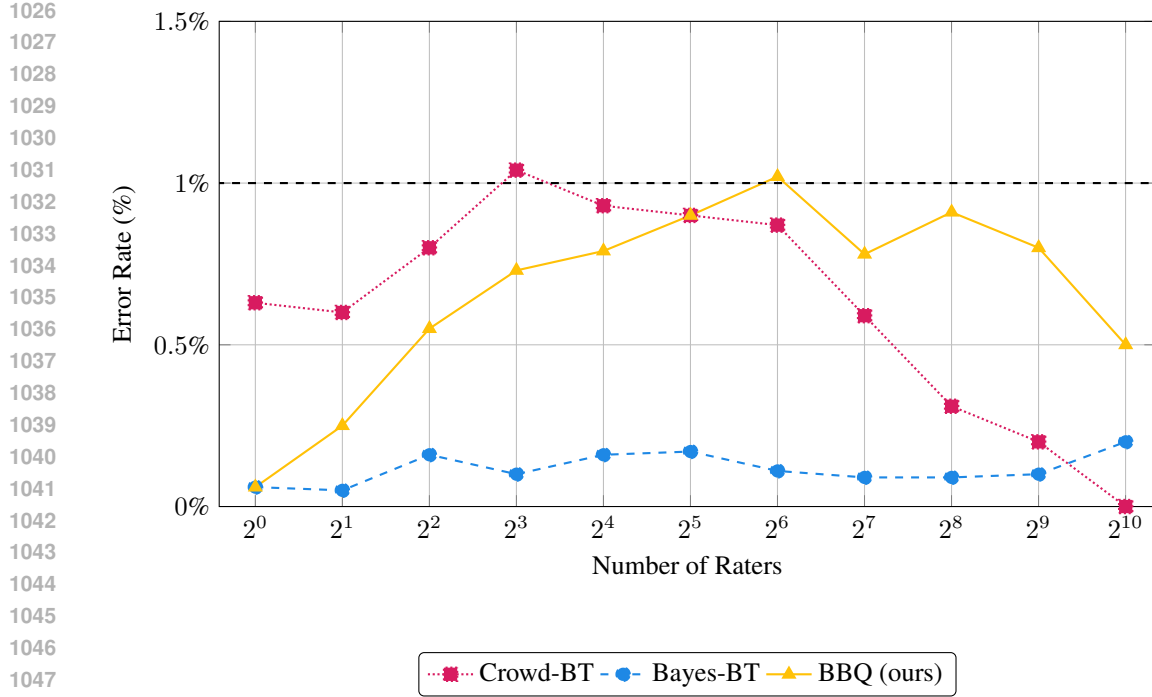


Figure 6: Type I error rate as a function of the number of raters. The dashed line indicates the expected error rate of 1%.

To evaluate how well these models estimate uncertainty, we conduct a controlled simulation experiment. We generate trials with two items of equal skill (50–50 win probability) and simulate pairwise comparison data using coin flips. For each trial, multiple raters (users) are simulated, and models are applied to estimate Elo scores and their associated uncertainty.

Formally, the null hypothesis H_0 states that the two items are equally strong. For each trial, we compute the 99% confidence (or credible) interval for each item’s skill estimate. A model is said to incorrectly reject H_0 if the confidence intervals do not overlap, indicating a statistically significant difference between items when none exists. The primary metric of interest is the frequency with which each model incorrectly concludes that the items are different, i.e., the observed Type I error rate.

We perform 10,000 trials, using 50 comparisons per rater, while varying the number of raters to assess how uncertainty estimates scale with the amount of data. This setup allows us to estimate the empirical Type I error rate for each model and compare it against the theoretical expectation of 1% at the 99% confidence level. As shown in Figure 6, Crowd-BT and BBQ exhibit Type I error rates close to the expected 1%, indicating that their uncertainty estimates are well-calibrated. In contrast, Bayes-BT is overly conservative, consistently producing lower error rates than expected, which suggests its credible intervals are not as well-calibrated for significance testing.

H VISUAL EXAMPLES

Visual examples of the binary comparisons used in our evaluation are shown in Figures 7 and 8. For each pair, we also display the predicted win probability (in percentage) of the method that generated the corresponding image. These examples are randomly sampled from the IHQ all dataset and are not cherry-picked. Note that the predicted probability depends solely on the ELO score of the generative method and is therefore independent of the specific image content.

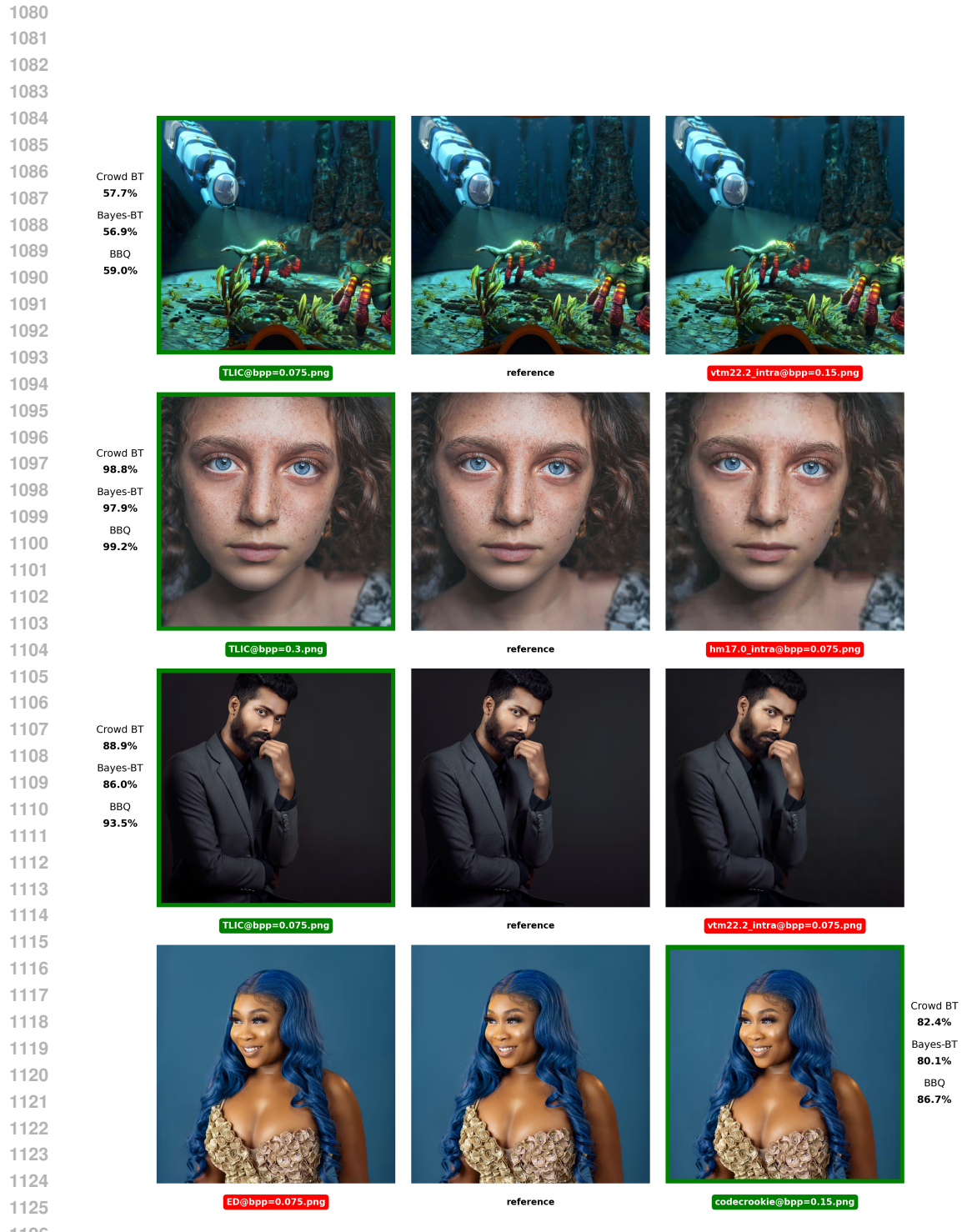


Figure 7: Example result from our binary comparison evaluation. The human-selected image is highlighted in green, and the non-selected image is shown in red. A table beside the selected image reports the predicted win probability of the corresponding generative method over its competitor. Note that these probabilities depend only on the ELO scores of the methods, not on the specific image content.

1131
1132
1133

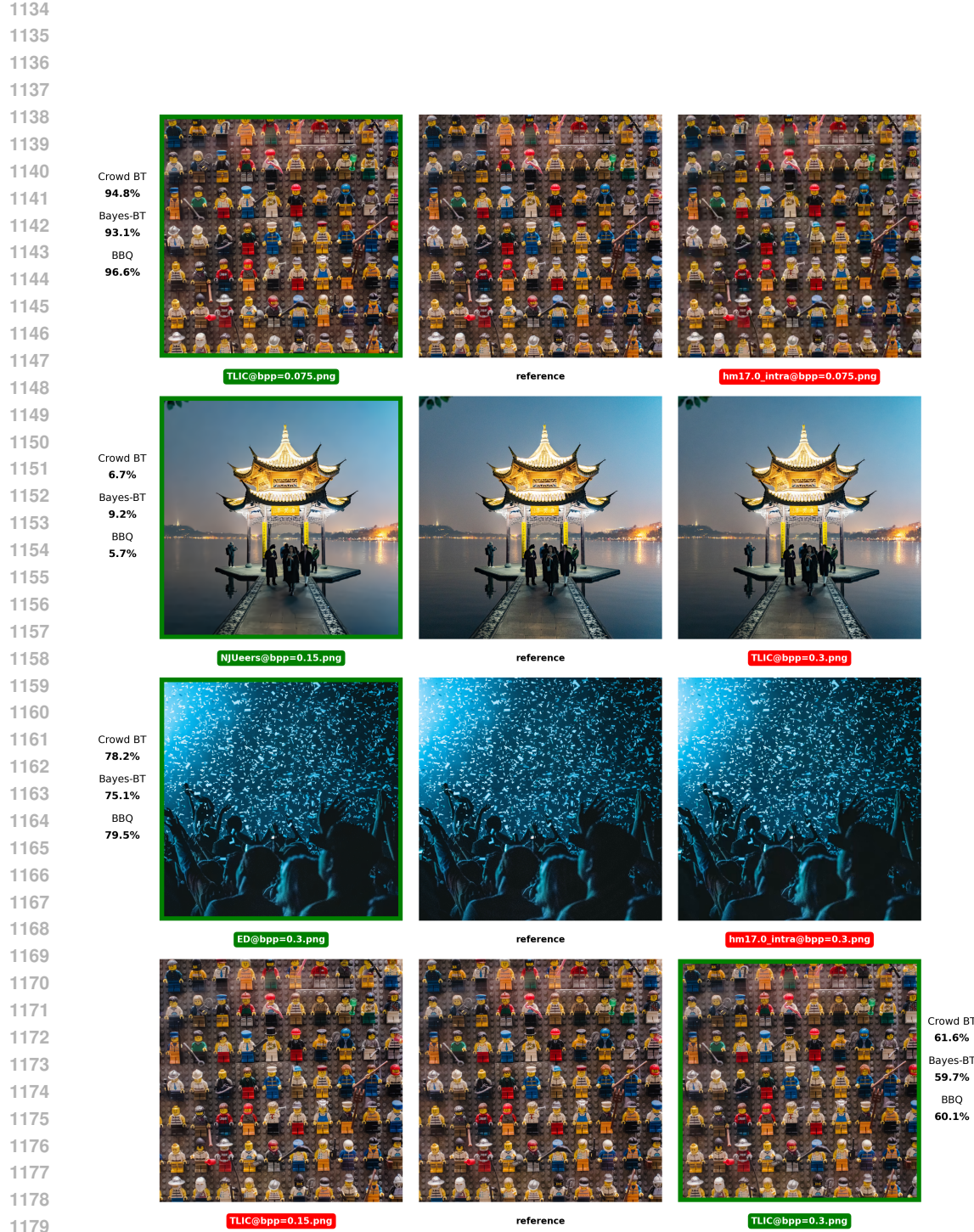


Figure 8: Example result from our binary comparison evaluation. The human-selected image is highlighted in green, and the non-selected image is shown in red. A table beside the selected image reports the predicted win probability of the corresponding generative method over its competitor. Note that these probabilities depend only on the ELO scores of the methods, not on the specific image content.